Plate anchors for floating offshore facilities: soil-anchor-floating system interactions

Ancrages plaques pour les installations flottantes en mer: interactions sol-ancrage-système flottant

Katherine Kwa & David White
Civil, Maritime & Environmental Engineering, The University of Southampton, United Kingdom, k.a.kwa@soton.ac.uk

ABSTRACT: The embedded plate anchor and mooring system is an efficient and versatile deep-water foundation solution. The capacity of the anchoring system is enhanced by the strength and weight of the surrounding soil which resists uplift of the plate. It is essential to have a reliable estimation of the uplift capacity that the plate anchor can provide for the variety of loads that are transmitted via the mooring lines to the anchoring system, and this capacity is enhanced by effects that are highlighted in this study – including consolidation and added mass during dynamic events. A systematic numerical study captures the effects of sustained loading and consolidation on the changing static anchor capacity and the effects of the added mass during rapid loading conditions on the dynamic anchor capacity. The results quantify the potential additional components of capacity that are currently overlooked in standard geotechnical design practice. It is also shown that these effects can be captured through simple analytical expressions, which can be used to represent the changing static and dynamic anchor capacities in a model of the full floating system behaviour.

RÉSUMÉ : Le système composé d'un ancrage plaque enfoncé dans le sol et d'un câble d'amarrage est un type de fondation efficace et polyvalent en eaux profondes. La capacité du système d'ancrage est améliorée par la résistance et le poids du sol qui empêche le mouvement vertical de la plaque. Il est nécessaire de pouvoir estimer précisément la résistance au soulèvement d'un ancrage plaque soumis à une gamme de chargements transmis par le système d'amarrage. Cette résistance est améliorée par plusieurs phénomènes présentés dans ce travail, notamment la consolidation du sol et la masse ajoutée sous chargement dynamique. Une étude numérique systématique a capturé les effets d'un chargement prolongé et de la consolidation du sol sur la résistance statique de l'ancrage, ainsi que les effets de la masse ajoutée sous chargement rapide sur sa résistance dynamique. Les résultats quantifient les possibles augmentations de capacité qui sont actuellement négligées dans le dimensionnement des ancrages. Il est aussi démontré que ces changements peuvent être capturés via de simples expressions analytiques, qui peuvent être utilisées pour représenter les changements de capacité statique et dynamique dans un modèle comprenant l'entièreté du system flottant.

1 INTRODUCTION

1.1 Offshore renewable energy: future development

The drive to decarbonise our energy supply to address climate change and meet the commitments of the Paris agreement has resulted in a rapid development and expansion of offshore renewable energy infrastructure. To reach net-zero, the UK has set a target of 75GW of offshore wind energy by 2050, which will require up to 7,500 additional wind turbines (CCC, 2019). The offshore wind renewable energy industry is also growing globally with an increasing number of countries planning pilot projects or full-scale development of commercial-scale offshore wind farms. Australia is one of the latest countries to enter the sector and is currently performing feasibility studies for three offshore wind projects including the Star of the South off the coast of Gippsland in Victoria (2.2 GW), Newcastle Offshore Wind in NSW (potential of ~10GW) and the Mid-West wind and Solar project south of Geraldton in WA (up to 1.1 GW) (MUA, 2020). Offshore wind feasibility studies performed in Australia have also identified a number of potential sites suitable for offshore wind that connect the offshore renewable energy resources along the coast to existing transmission lines, population and industry (Figure 1).

Figure 2: Potential areas for offshore wind development (MUA, 2020)

1.2 Offshore renewable energy: Ocean challenges

The offshore renewable energy industry is developing new solutions that will enable floating renewable energy facilities to operate further offshore in deeper waters where stronger wind resources can be harnessed. Developments in the mooring and foundation system technologies are required to unlock large scale commercialisation for floating offshore wind (ETIPWIND, 2020a, 2020b). In traditional offshore oil and gas facilities geotechnics accounts for typically 0.5 to 3% of project costs and the main asset is usually a single, large manned structure engineered with high levels of conservatism (Figure 2, left side). However, different emergent types of infrastructure are required to enable, commercial scale offshore renewable energy facilities (Figure 2, right side). This infrastructure targets a spatially-spread resource and require multiple similar structures and foundations with lengthy interconnections. The resulting geotechnical costs are forecasted to be significantly higher, at 15 to 30% of the project value of offshore floating renewable energy infrastructure (Carbon Trust, 2015). Therefore, there is a significant opportunity of unlocking the embedded conservatism in understanding and modelling of offshore geomaterials through innovation and optimization. However, there is also an inherent difficulty in innovating in the ocean space, since field testing is risky and high in cost.

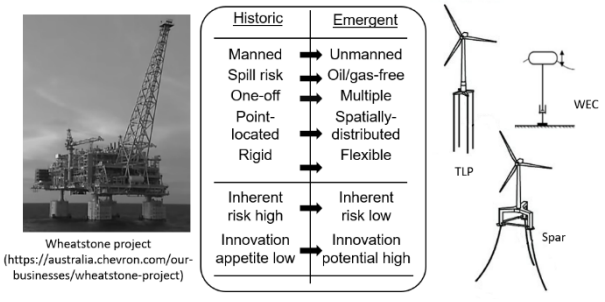

Figure 1: Design challenge contrasts of past oil and gas facilities and future offshore renewables facilities

1.3 Anchoring systems

The embedded plate anchor is a versatile and efficient soft soil, deep-water foundation solution for offshore floating renewable energy structures. It can be installed or embedded into the seabed by drag-embedment, free-fall, screwing or via a suction anchor (Randolph & Gourvenec 2017, Aubeny 2017, O'Loughlin et al. 2017). The mooring tension is then applied via a chain or cable system, directly to the plate or an attached shank (or in the case of a screw anchor, to a shaft at mudline) (Figure 3) and the resulting anchor capacity depends on and can be enhanced by the surrounding soil.

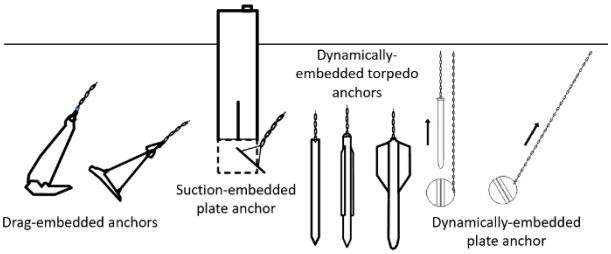

Figure 3: Anchoring systems for offshore floating systems

1.4 Anchor capacity: conventional capacity methods

This study explores the capacities of anchoring systems embedded in undrained clays. It is essential to have a reliable estimate of the current available capacity that the anchoring system can provide for the range of actions that the offshore floating facility is subjected to over its operational lifetime. The anchor loads transmitted via mooring lines to the anchoring system depend on the variable metocean and operational conditions and can be broadly classified as (i) long-term loads such as sustained, transient, cyclic or episodic or (ii) rapid or short-term dynamic loads including snatch loads. The factored design capacity (Q_{fac}) for undrained loading of a plate anchor is written as (DNV, 2002):

$$Q_{fac} = \frac{1}{\gamma_m} N_c s_u A_p \qquad (1)$$

where A_p is the plate area and the three factors that control anchor capacity are (i) γ_m a resistance factor (γ_m >1) for uncertainty, (ii) N_c is the bearing factor and (iii) s_u is the undrained strength relevant to the loading. Various parameters or effects can influence the values of N_c and s_u, however our approach is to treat N_c and s_u independently such that s_u is the volume-averaged strength of the failing soil and N_c is the ratio between the mean bearing stress (Q/A_p) and s_u. This is based on the observation that N_c and s_u are independent for surface plate foundations subjected to consolidation and therefore, changes in the distribution of s_u do not lead to changes in N_c (O'loughlin et al, 2017; Stanier & White, 2017).

1.5 Anchor capacity: opportunities for improvement

The conventional capacity methods overlook three sources of potential capacity enhancement as follows:

(i) long term change in available strength, s_u
(ii) short term change in available strength, s_u due to viscous effects
(iii) added mass effects

These effects are briefly described below, and analysed in sequence in the body of the paper.

Under long term loading conditions, the anchor capacity can change over the design life of the floating facility due to shearing and consolidation of the surrounding seabed, resulting in changes in seabed stiffness and strength (Gourvenec, 2020, Laham et al., 2020). This can result in rises in the long-term capacity of the embedded plate anchor (Han et al. 2016, Zhou et al 2019, Kwa & White, 2020) in a similar manner to the established response of surface foundations and pipelines (e.g. Bransby, 2002, Gourvenec et al. 2014; Smith & White, 2014, Cocjin et al. 2014, 2017; Lai et al., 2020). However, these long-term or whole-life increases in capacity are not typically considered in conventional geotechnical foundation capacity analysis.

Viscous rate effects can also have a positive effect on the shear strength of the soil, depending on the strain rate as defined below (Randolph, 2004)

$$s_u = s_{u0}\, max\left[1, 1 + \mu' \sinh^{-1}\frac{\dot{\gamma}}{\dot{\gamma_{ref}}}\right] \qquad (2)$$

where s_{u0} is the undrained shear strength defined at a slow or static strain rate, μ' is a rate parameter, typically taken as 0.1 (i.e. 10% extra strength per increment of strain), $\dot{\gamma}$ is a representative strain rate in the soil and $\dot{\gamma}_{\mathrm{ref}}$ is a strain rate associated with failure selected during design. Traditional mechanical analogues define viscous rate effects using a dashpot with a resistance that is linearly proportional to the velocity. In geotechnics, it is recognized that the additional resistance is proportional to the log of the strain rate or velocity. Equation (2) has a similar form to the log function, but with a smooth transition to the minimum strength, s_{u0}, rather than the abrupt cut-off of a minimum s_{u0} in the log approach. Equation (2) is therefore useful to capture increases in undrained soil strength, and therefore anchor capacity, for different loading frequencies.

Under rapid loading events like snatch loads, which can have periods ~10 times shorter than the wave itself (e.g. Hann et al. 2015, Lind et al. 2016), extra anchor capacity is also created from mobilising the mass of the soil surrounding the plate. This added soil mass can be described by the hydrodynamics 'added mass term', which is well recognised in fluid mechanics (e.g. Lamb 1895, Morison et al 1950, Sarpkaya & Isaacson 1981) and is routinely considered in the dynamic motion of floating structures and mooring lines. This extra dynamic anchor capacity is also not considered in conventional geotechnical capacity analysis. Allowing for these long-term or static and rapid dynamic loading soil-anchor interactions can have a beneficial design outcome, offering opportunities for more efficient anchoring systems including reductions in anchor size. These soil-anchor interactions should also be integrated into the analysis of the connected floating structure to predict the full floating response of the infrastructure and optimally design and manage the facility. However, typical fluid-structure interaction models model the connection of the structure to the seabed as a pin connection and the soil-anchor interactions are not included.

1.6 Aim and outline of paper

This paper is part of the UK's Offshore Renewable Energy (ORE) Supergen Hub project. One topic of research within the hub is ORE design, with an emphasis on floating systems. An aspect of this work is concerned with more realistic modelling of anchor-seabed interaction, ultimately to add the anchorage into the full analysis of floating offshore renewable energy infrastructure. The aim is to enable integration of the soil-anchor interactions into mooring analyses in a simple and practical way, while unlocking the full potential capacity. This will be achieved by using spring-slider and added mass elements to represent the different soil-anchor interactions as shown in Figure 4.

This study presents and discusses results from numerical studies that characterise the static increases in plate anchor during sustained loading and the dynamic soil added mass term mobilised under rapid snatch loading conditions. These static and dynamic soil-anchor effects are also summarised into analytical expressions, that can be used to represent the spring-slider changing static anchor capacity relationships and the dynamic added mass terms in a simple way that can be easily adopted into models that analyse the full floating behaviour of offshore infrastructure

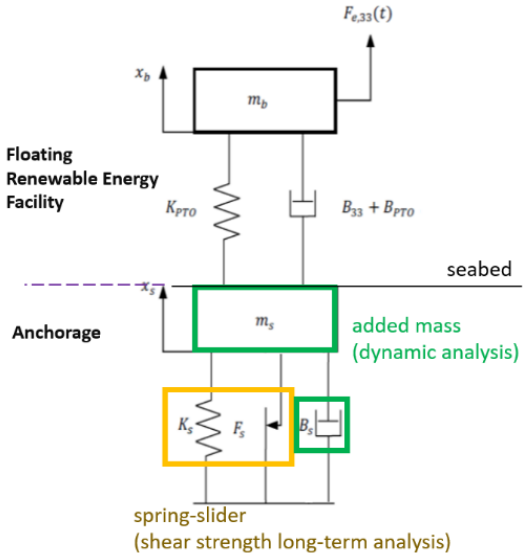

Figure 5: Schematic of anchorage, consisting of spring-slider and added mass elements, connected to the floating renewable energy facility

2 STATIC LONG-TERM ANCHOR CAPACITY

2.1 Model Properties

To characterise changes in static anchor capacity, small strain finite-element analyses were performed in PLAXIS 2D. The modified Cam clay critical state model within PLAXIS was adopted to investigate the coupled effects of consolidation and strength gain in the soil around an embedded plate anchor subjected to sustained loading and pull out. A rigid circular plate anchor with rough interfaces was considered. Soft normally consolidated clay conditions were modelled. The soil was represented with the PLAXIS default 15-noded triangle elements which use fourth-order interpolation for displacements and their numerical integration involves twelve Gauss points. The modelled strength profile is typical of soft seabed conditions (Randolph & Gourvenec 2017).

An initial benchmarking exercise was performed to validate the PLAXIS results where the monotonic embedded plate anchor capacities were compared with the well-established analytical solutions described in Martin & Randolph (2001) and Martin (2003) to confirm that the numerical simulation is accurate for undrained collapse calculations. More details of the benchmarking exercise can be found in Kwa & White (2020b).

2.2 Consolidation effects

The effect of consolidation under a sustained preload (V_p) in the range of V_p/V_{uu} from 0.05 to 0.65 (where V_{uu} is the undrained uniaxial vertical bearing capacity), on the final consolidated undrained vertical bearing capacity (V_{cu}) of the embedded plate anchor was investigated. The increase in consolidated capacity from static preloading of an embedded circular plate anchor was investigated. Each analysis followed the same principal steps:

(i) establishment of the in-situ stress conditions with a nominal surface surcharge of 10kPa to prevent a zero-stress state at the mudline, followed by a period of consolidation to allow the soil to reach equilibrium
(ii) preloading the foundation V_p, applied as an upward point load at the middle of the foundation
(iii) a consolidation period
(iv) a vertical upward displacement causing undrained uniaxial bearing failure, mobilising V_{cu}

The resulting gains in the embedded anchor capacity were compared to surface footing solutions established in Gourvenec et al. (2014). The relationship set out by Gourvenec et al (2014) describes the gains in capacity for a surface footing as proportional to the preload level

$$G = 1 + RN_c f_{su} P \quad (3)$$

where G represents the gain in capacity (V_{cu}/V_{uu}), R is the ratio $(s_u/\sigma'_{v0})_{NC}$ following Schofield & Wroth (1968), N_c is the bearing capacity factor, f_{su} is the scaling factor (typically ~0.45) from Gourvenec et al. (2014) and P is the preload level (V_p/V_{uu}). The typical value of f_{su}=0.45 means that a sustained preload of V_p leads to a gain in capacity of ~0.8 V_p through consolidation.

Unlike in the surface footing case, the gains in embedded anchor capacity varied non-linearly with preload level and were lower than in the surface footing case (Figure 5). There are two distinct regions of response. At low loads, the best fit scaling factor was f_{su}=0.075, whereas above a threshold of P~0.5, the gain is more significant and f_{su}=0.4. This was a result of the complex soil-plate anchor interactions in the soil regions above and below the plate. As the plate was pulled upward, the soil above the plate compressed and strengthened, while the soil below the plate was unloaded. The flow of soil and the mobilised failure mechanisms in the soil around the plate also varied with the different preloads that were applied. At a preload fraction P=0.5, there was a transition in the mobilised failure mechanisms between a two-way mechanism, where soil above and below the plate were involved in the failure mechanism as soil flowed from above to below the plate, to a one-way mechanism, where a gap formed between the soil and underside of the plate and all the uplift force was resisted by the soil above the plate. This transition was observed when comparing the different undrained strength profiles that develop around the plate at P<0.5 and P>0.5 as shown in Figure 5.

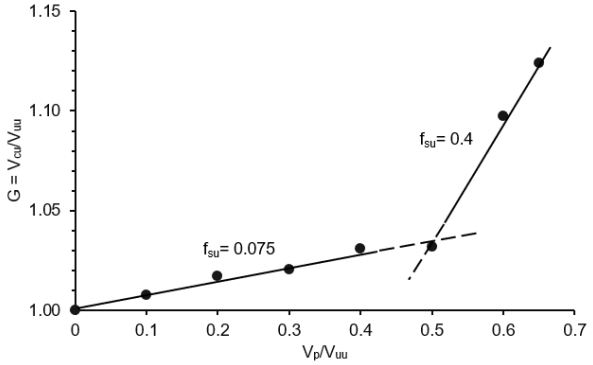

Figure 4: Normalised gains in bearing capacity after consolidation under normalised preload for deeply embedded circular plates

The development of the different two and one-way failure mechanisms was also evident upon inspecting the fundamental soil mechanics behind these different soil and plate interactions and mobilised failure mechanisms when varying preloads are applied. These are examined in more detail in Kwa & White (2020b) where changes in undrained strength and void ratio, the associated effective stress paths and the average total, effective and water pressures observed in the soil regions above and below the embedded plate when different preloads are applied, are presented and discussed.

2.3 Spring-slider relationship

These increases in static anchor capacity as a result of long-term sustained preloading can be captured by changing the spring slider parameters via a relationship of this form:

$$K_s = GK_{s,init} f(t) \quad (5)$$

where $K_{s,init}$ is the initial spring slider relationship before any strengthening occurs and $f(t)$ is a function dependent on time (t) and the gain in static capacity (G) is linked to the preload level. From the numerical results shown earlier, this spring-slider relationship in the whole-life full floating analysis can result in up to a 12% increase in static anchor capacity for combination of soil parameters used in this study. However, further increases in static capacity are expected if the sustained loads include cyclic components and background consolidation. Such gains in soil strength have been observed in a suite of novel episodic, cyclic direct simple shear (DSS) tests described in Laham et al., (2020), and the prediction model validated by these tests shows the potential for an approximate doubling in soil undrained strength as a result of this effect, consistent with critical state theory.

3 DYNAMIC ANCHOR CAPACITY

3.1 Analytical Solutions

To quantify the additional dynamic anchor capacity from mobilising the added soil mass around an embedded plate anchor, conventional upper bound geotechnical collapse mechanisms around an embedded plate were assumed. The general approach outlined here and in more detail in Kwa et al. (2020a) can also be applied to shallow or piled foundations, using the geometry of any mobilised failure mechanism to evaluate the added mass.

In undrained soils, the upper bound theorem is used to define a kinematically-admissible collapse mechanism for an embedded plate. Rigid sliding blocks of soil flow around the plate moving at a velocity (v_f). The internal work dissipation rate on each sliding plane, is the product of the shear forces and relative velocities on the plane. Equating the work input to the dissipation gives the capacity due to the soil strength:

$$F_{su} = N_c s_u B \qquad (6)$$

Solving the work equation in plane strain for an embedded plate in homogenous clay results in N_c=3π+2 (Meyerhof 1951, Rowe & Davis 1982, Martin & Randolph, 2001).

Under rapid loading, at failure, additional work is required to accelerate the soil mass within the mobilized failure mechanism according to Newton's 2nd Law. The acceleration varies throughout the mechanism and the net effect is an additional component of resistance $F_{AM} = m_{AM}a$ where a is the acceleration of the plate and m_{AM} is a representative added mass and this term can also be derived from the collapse mechanism as described later. Therefore, the total resistance force (F) on the plate after F_{su} is exceeded is

$$F = F_{su} + F_{AM} \qquad (7)$$

In hydrodynamics, fluid flow around an accelerating plate is a classical problem (Lamb, 1895). The added mass term is found by integrating the velocities over the flow field caused the accelerating body and solutions exist for various rigid bodies (Newman, 2018). By using the potential flow solutions for the velocity field, the forces to accelerate a plane strain thin plate, or strip, of width B or a thin circular plate of diameter B in the axisymmetric case, are:

$$F_{AM} = m_{AM}a = \frac{\pi}{4}\rho B^2 a \qquad (8a)$$

$$F_{AM} = m_{AM}a = \frac{1}{3}\rho B^3 a \qquad (8b)$$

It is useful to define the dimensionless hydrodynamic added mass coefficient as $N_{AM,2D}$=$m_{AM}/\rho B^2$ or $N_{AM,3D}$=$m_{AM}/\rho B^3$ for the 2D plane strain and 3D axisymmetric cases and so $N_{AM,2D}$=$\pi/4$ and $N_{AM,3D}$=1/3 respectively. This same approach is used by Kwa et al. (2020) to derive added mass terms for geotechnical collapse mechanisms, derived from limit plasticity. The adopted approach allows added mass resistance to be derived for the types of failure mechanism that are used in conventional geotechnical design. Similarly, conventional bearing capacity factors can be derived by considering the dissipated work within a flow field derived using a fluid mechanics approach, such as inviscid flow. The resulting N_c and N_{AM} factors from Kwa et al. (2020a) for a circular plate anchor are shown in Table 1 and the total force (F) on a rapidly moving plate anchor can therefore be written as

$$F = N_c s_u B + N_{AM}\rho B^2 a \qquad (9)$$

Table 1: Summary of bearing capacity factors and added mass coefficients for a circular plate

Coefficients	N_c	$N_{AM,3D}$
Inviscid flow	16.198[e], 14.842[f]	0.33
Analytical UB[#]	13.11[a], 12.42[b]	-
OxLim UB	13.13[a], 12.435[b]	0.548[a], 0.599[b]

[#]Martin & Randolph (2001), [a, b] Rough and smooth analyses, [e, f] Tresca, Von Mises

3.2 Contributions from N_{AM} and N_c

The calculated value of N_{AM} from the geotechnical collapse mechanism is significantly larger than from the inviscid flow field and this is a result of the different flow mechanisms that develop. In inviscid fluids, there is negligible shear resistance within the material and the flow field develops such that the added mass term is minimised. However, soil has shear resistance and the resulting optimal flow field minimises shearing resistance. The resulting mechanism in soil is larger resulting in a higher added mass. Therefore, these failure mechanisms that are exact for inviscid flow and rigid plastic flow represent extremes of the soil response across the potential range of loading rates. The different contributions of the shear strength and added mass to the total resistance are shown in Figure 6 across the range of dimensionless group $s_u/B\rho a$, which represents the balance between shear strength and inertia forces.

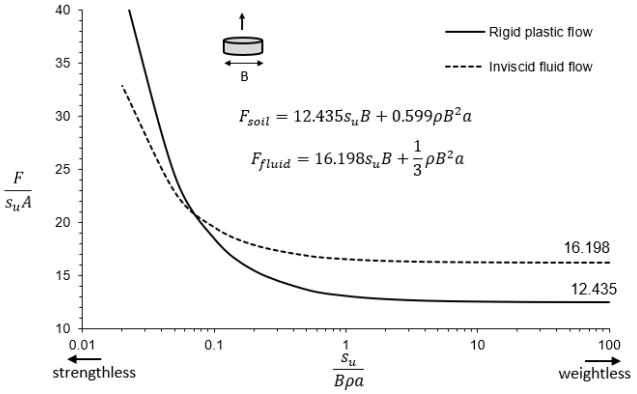

Figure 6: Contributions of shear strength and added mass of the material with respect to the dimensionless group $s_u/B\rho a$ for a circular disc

At high values of $s_u/B\rho a$, the shear strength term dominates, and the soil can be considered as weightless in the limit $s_u/B\rho a \to \infty$, so the uplift capacity approaches the rigid plastic solution. Under these conditions, the acceleration applied to the anchor and surrounding soil is small and therefore, increases in the static capacity (F_{su}) from sustained loads as discussed previously can be applied. Conversely, at low $s_u/B\rho a$, the added mass term dominates and, in the limit, $s_u/B\rho a \to 0$ the soil has no shear strength and is subjected to high accelerations. The combined resistance from the bearing capacity (N_c) and added mass coefficients (N_{AM}) of the inviscid and rigid plastic solutions are consistent with this transition. At high $s_u/B\rho a$ the rigid plastic mechanism offers lower total resistance and

therefore is the optimal failure mechanism, whereas at low $s_u/B\rho a$ the inviscid flow solution is lower. This transition occurs at $s_u/B\rho a$ ~1 for plane strain, and ~0.08 for axisymmetry.

In practice, the optimal mechanism that is mobilised could involve a mixture of the rigid plastic and inviscid flow fields, which are superposable. The transition between rigid plastic, inviscid flow, or a mixture, is likely to be smooth, similar to experimental observations for steady flow around a cylinder in soft soil (Sahdi et al. 2014).

3.3 Application of added mass and viscous effects

The influence of added mass and viscous effects for a typical snatch load design event represented by a force impulse (F_{load}) is demonstrated here. A summary of the parameters and values used in this example is included in Table 2.

Table 2. Summary of parameters used in example application

Input Parameters	Value	Units
Plate properties		
Plate diameter, B	5	m
Soil Properties		
Soil density, ρ	2300	kg/m^3
Undrained shear strength s_{u0}	10	kPa
Geotechnical capacity		
Bearing factor, N_c	13.11	-
Geotechnical capacity F_{su}	2574	kN
Added mass resistance		
Added mass coefficient N_{AM}	0.548	-
Added mass	178×10^3	kg
Rate parameter μ'	0.1	
Design strain rate $\dot{\gamma_{ref}}$	0.02	

The impulse load F_{load} is

$$F_{load} = F_{min} + (F_{max} - F_{min})\left(\frac{sin\left(\frac{t-\alpha}{T}\right)}{\frac{t-\alpha}{T}}\right) \quad (10)$$

and is shown in Figure 7 where F_{min} represents the superposition of the steady static component (F_{su}) of the mooring load that does not change under the short time scale of the rapid dynamic loading event, and the viscous rate effects (B_s), which result in increases in s_u according to Equation 2 and activates when the peak of the design wave load (F_{load}) exceeds the static anchor capacity (F_{su}). F_{max} is the peak load, varying with time, t, offset by α, with T being the period of the dynamic loading event (set to 10 seconds in this example application). When F_{load} exceeds F_{su} and the plate moves, Newmark's β method is used to calculate the resulting velocity, acceleration and displacement responses with and without considering the added soil mass term and viscous rate effects, as shown in Figure 8. F_{AM}, is the extra resistance force from the acceleration of the soil mass involved in the failure mechanism during the impulse load.

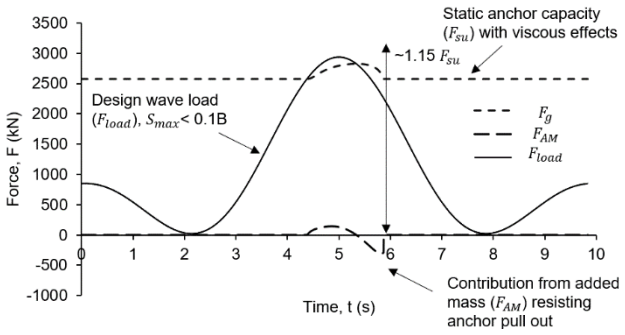

Figure 8. Summary of forces acting on the embedded plate anchor during an example impulse snatch load with a period of 10 seconds

The anchoring system withstood a peak load that is ~15% greater than the geotechnical static capacity, due to the contribution from added mass and viscous effects, where failure of a plate anchor is defined at a displacement (S_{max}) of 10% of the plate diameter. In Figure 8, the velocities (v), accelerations (a) and displacements experienced by the plate significantly decreased when the added mass and viscous of the surrounding soil were considered. The added mass and viscous effects each contributed ~7.5% of extra capacity to the allowable design load for the set of parameters used in this example. This demonstrates that both the added mass and viscous effects can significantly enhance the anchor capacity available to resist dynamic loads, beyond the geotechnical capacity that is typically used in practice.

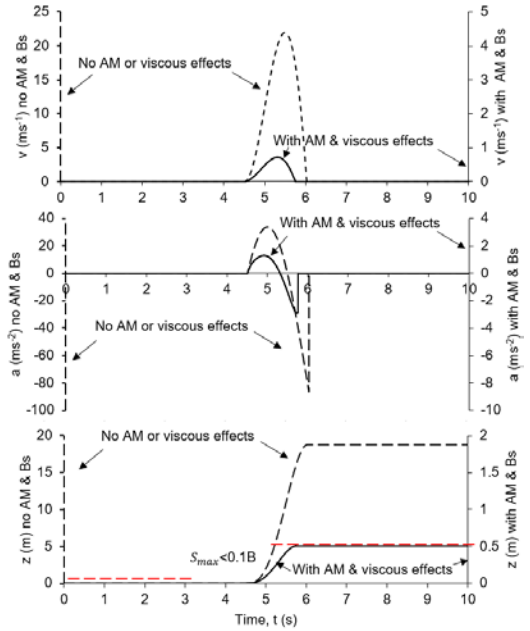

Figure 7. Comparison of anchor movements during an example snatch load (period=10 s) with and without the added mass and viscous effects

The extra capacity from the added mass also increases for more severe snatch loads with shorter periods (e.g. 1 second) of similar magnitude, where the accelerations mobilised in the soil become significantly larger and can contribute up to 70% extra dynamic anchor capacity as demonstrated Figures 9 and 10 However, shorter period snatch loads are also associated with smaller contributions from the viscous effect, which is activated over a shorter period of time and results in smaller increases in s_u. It is possible that these contributions from the added mass and viscous soil effects which are overlooked in design, are partly responsible for mooring systems failures being primarily due to mooring lines breaking, rather than anchors pulling out (Ma et al. 2019). This is why it is important to include the dynamic effects from the added mass and viscous effects, represented in Figure 4 as m_s and B_s, in anchorage and couple the anchor-soil effects with the mooring analysis to understand the full floating behaviour of the of the connected floating infrastructure.

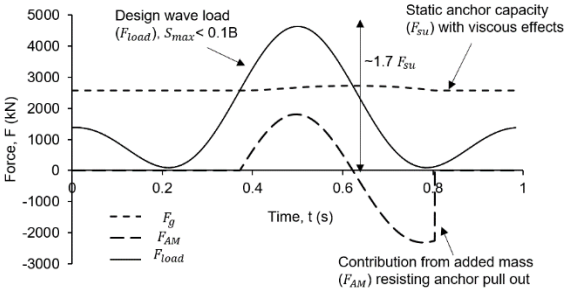

Figure 9 Summary of forces acting on the embedded plate anchor during an example impulse snatch load with a period 1 second

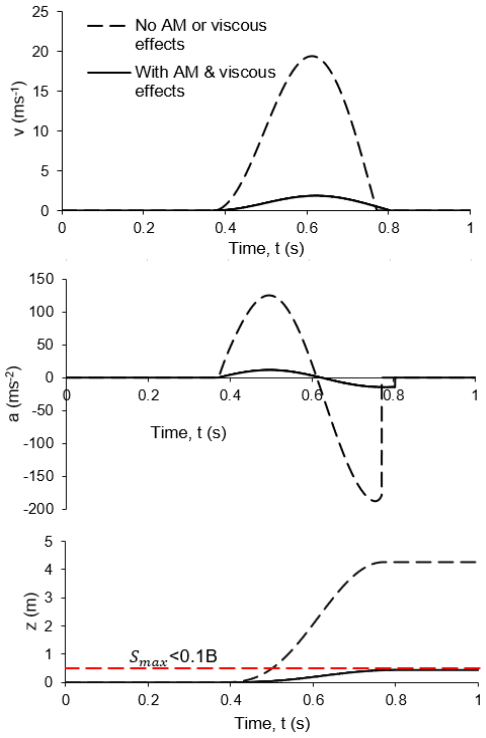

Figure 10 Comparison of anchor movements during an example snatch load (period=1 s) with and without the added mass and viscous effects

4 CONCLUSIONS

Significant increases in embedded anchor capacity can result from modelling the static and dynamic soil-anchor effects associated with

(i) the long-term changes in s_u when consolidation induced changes can occur during the application of sustained or episodic cyclic loads

(ii) the short-term changes in s_u due to viscous effects

(iii) the added mass effects during brief loading events like snatch loads

These static and dynamic soil-anchor effects are overlooked in conventional design. This study has analysed these static and dynamic soil-anchor effects and summarised them into simple analytical expressions that can be used to describe spring-slider and added mass relationships. These spring-slider and added mass relationships can be easily adopted as anchorage and integrated into existing models to describe and improve our understanding of the full floating behaviour of offshore renewable energy structures.

5 ACKNOWLEDGEMENTS

The authors acknowledge support from the EPSRC Supergen Offshore Renewable Energy Hub (EP/S000747/1) and Royal Academy of Engineering Chair in Emerging Technologies in Intelligent and Resilient Ocean Engineering.

6 REFERENCES

Aubeny, C., (2017). Geomech. of Marine Anchors. CRC Press

Acosta-Martinez, H. E. & Gourvenec, S. M. (2006). One-dimensional consolidation tests on kaolin clay. COFS, University of Western Australia, Crawley, Australia, research report GEO: 06385.

Bransby, M.F. (2002) The undrained inclined load capacity of shallow foundations after consolidation under vertical loads. In Num. Models in Geomech: Proceed. 8th Int Symp. Rotterdam, Netherlands, Balkema

Carbon Trust (2015). Floating Offshore Wind: Market & Technology Review, Carbon Trust.

Climate Change Committee (CCC), (2019). Net Zero Technical Report, Net Zero Reports, 2 May 2019

Cocjin M., Gourvenec S., White D.J and Randolph M.F. (2014) Tolerably mobile subsea foundations – Observations of performance. Géotechnique 64(11): 895-909.

Cocjin M., Gourvenec S., White D.J and Randolph M.F. (2017) Theoretical framework for predicting the response of tolerably mobile subsea installations. Géotechnique 67(7): 608-620

DNV (Det Norske Veritas) (2002). DNG-RP-E02: Recommended practices: design and installation of plate anchors in clay. DNV

ETIPWIND (2020a) European Technology & Innovation Platform on Wind Energy Roadmap.

ETIPWIND (2020b) Floating offshore wind delivering climate neutrality, ETIPWIND

Gourvenec S. (2020) Whole-life geotechnical design: What is it? What's it for? So what? And what next? Proc. 4th ISFOG. 2021, Proc. Aug 2020. Austin, Texas, USA

Han, C., Wang, D., Gaudin, C., O'Loughlin, C.D. and Cassidy, M.J., (2016). Behaviour of vertically loaded plate anchors under sustained uplift. Géotechnique, 66(8), pp.681-693.

Hann, M., Greaves, D. and Raby, A., (2015). Snatch loading of a single taut moored floating wave energy converter due to focussed wave groups. J. Ocean Eng., 96, pp.258-271.

Lai Y., Wang L., Hong Y. and He B. (2020) Centrifuge modeling of the cyclic lateral behavior of large-diameter monopiles in soft clay: Effects of episodic cycling and reconsolidation. J. Ocean Eng., 200, 2020, 107048,

Laham, N., Kwa, K.A., White, D.J. & Gourvenec, S. (2020), Episodic direct simple shear tests to measure changing strength for whole-life geotechnical design, Geotechnique Letters

Kwa, K.A., Weymouth, G., White, D.J., Martin., C.M. (2020a). Analysis of the added mass term in soil bearing capacity problems, Geotechnique Letters

Kwa, K.A. & White, D.J. (2020b), Enhanced capacity of plate anchors due to consolidation under sustained load, Geotechnique

Lamb, H., (1895). Hydrodynamics. Cam. University Press.

Lind, S.J., Stansby, P.K. and Rogers, B.D., (2016). Fixed and moored bodies in steep and breaking waves using SPH with the Froude–Krylov approximation. J.Ocean Eng. & Marine Energy, 2(3), pp.331-354.

Ma K.T., Luo Y., Kwan, T. & Wu, Y. (2019). Mooring system reliability. Mooring System Eng. for Off. Struct. 255-279.

Maritime Union of Australia (MUA). 2020. Building offshore wind from https://www.mua.org.au/building-offshore-wind-australia retrieved 27/11/2020

O'Loughlin, C.D., White, D.J. and Stanier, S.A., (2017). Plate Anchors for Mooring Floating Facilities–A View Towards Unlocking Cost and Risk Benefits. In Offshore Site Investigation Geotechnics 8th Int Conf Proc. (Vol. 978, No. 986, pp. 978-986). Society for Underwater Technology.

Meyerhof, G.G., (1951). The ultimate bearing capacity of foundations. Geotechnique, 2(4), pp.301-332.

Newman, J.N., (2018). Marine hydrodynamics. MIT press.

Randolph, M., 2004. Characterisation of soft sediments for offshore applications, In Proc. Geotech & Geophys. Site Charac., Rotterdam.

Randolph, M. and Gourvenec, S., 2011. Offshore geotechnical engineering. CRC press.

Rowe, R. K., & Davis, E. H. (1982). The behaviour of anchor plates in clay. Geotechnique, 32(1), 9-23.

Sahdi F., Gaudin C., White D.J. Boylan, N.P. & Randolph M.F. (2014). Centrifuge modelling of active slide-pipeline loading in soft clay Géotechnique, 64(1):16-27

Sarpkaya, T.; Isaacson, M. (1981), Mechanics of wave forces on offshore structures, New York: Van Nostrand Reinhold

Schofield, A., & Wroth, P. (1968). Critical state soil mechanics. McGraw-hill.

Smith V. B. and White D. J. (2014) Volumetric hardening in axial pipe soil interaction. In Proc. Offshore Technology Conference Asia, OTC ASIA 2014: Meeting the Challenges for Asia's Growth (Vol. 2, pp. 1611-1621).

Stanier, S.A. and White, D.J., (2018). Enhancement of bearing capacity from consolidation: due to changing strength or failure mechanism?. Géotechnique, 69(2), pp.166-173.

Stewart, D. P. (1992). Lateral loading of piled bridge abutments due to embankment construction. PhD thesis, The University of Western Australia, Crawley, Australia

Yasuhara, K., & Andersen, K.H. (1991) Recompression of normally consolidated clay after cyclic loading. Soils & Found. 31(1), 83-94

Zhou, Z., O'Loughlin, C. D., White, D. J., & Stanier, S. A. (2019). Improvements in plate anchor capacity due to cyclic and maintained loads combined with consolidation. Géotechnique, 1-18.